[4]J. A. Simpson, in Proceedings of the International Conference on Cosmic Rays, Jaipur, India, 1963, edited by R. R. Daniel et al. (Commercial Printing Press, Ltd., Bombay, 1964-1965), Vol. 2, p. 155.

[5]G. Gloeckler, J. Geophys. Res. 70, 5333 (1965).

[6]V. K. Balasubrahmanyan, D. E. Hagge, G. H. Ludwig, and F. B. McDonald, in Proceedings of the Ninth International Conference on Cosmic Rays, London, 1965 (The Institute of Physics and the Physical Society, London, 1966), Vol. 1, p. 427.

[7]R. Silberberg, Phys. Rev. (to be published); and references therein.

[8]J. R. Jokipii, to be published.

[9]P. J. Coleman, thesis, Institute for Geophysics and Planetary Physics, University of California, Los Angeles, 1966 (unpublished).

[10]G. L. Siscoe, private communication.

[11]C. Y. Fan, G. Gloeckler, K. C. Hsieh, and J. A. Simpson, Phys. Rev. Letters 16, 813 (1966).

[12]C. Y. Fan, G. Gloeckler, and J. A. Simpson, in Proceedings of the Ninth International Conference on Cosmic Rays, London, 1965 (The Institute of Physics and the Physical Society, London, 1966), Vol. 1, p. 109.

[13]See University of Chicago Climax neutron monitor daily average intensity given in National Bureau of Standards Central Radio Propagation Laboratory, Reports Nos. CRPL-F 234-255, Pt. B. Boulder, Colorado, 1964, 1965 (unpublished).

[14]E. N. Parker, Planetary Space Sci. 13, 9 (1965).

[15]E. N. Parker, Planetary Space Sci. 14, 371 (1966).

[16]W. I. Axford, Planetary Space Sci. 13, 115 (1965).

[17]The computation of the diffusion coefficient in Ref. 8 requires that the change in mean field $\boldsymbol{B}_0$ be small over the scattering mean free path $\lambda \sim \kappa_{\parallel}/c\beta$. For 100-MeV protons, $\lambda \sim 10^{12}$ cm, whereas the scale length of the field beyond 1 A.U. is greater than 1 A.U. $\sim 1.5 \times 10^{13}$ cm so that the assumption is reasonably well satisfied.

[18]We have plotted the data at a weighted median energy $\langle T\rangle = 450$ MeV which is obtained from

$$\int_{50}^{\langle T\rangle} dE\left(\frac{j}{R\beta}\right) = \int_{\langle T\rangle}^{\infty} dE\left(\frac{j}{R\beta}\right).$$

Here j is the differential proton spectrum measured at Earth as given in Ref. 7. The value of $\langle T\rangle$ is not very sensitive to the form of the weighting function. The contribution of helium to the Geiger-Müller rate was neglected since it only amounts to 10-15% of the total.

[19]The fractional change in the Climax neutron monitor intensity is multiplied by 2.0 (private communication from J. A. Simpson) to deduce the primary proton variation. These points are plotted at the detector threshold of 3.0 GV because of the sharply falling spectrum.

[20]K. Nagashima, S. P. Duggal, and M. A. Pomerantz, Planetary Space Sci. 14, 177 (1966).

[21]I. V. Dorman and L. I. Dorman, in Proceedings of the Ninth International Conference on Cosmic Rays, London, 1965 (The Institute of Physics and the Physical Society, London, 1966), Vol. 1, p. 97.

[22]W. R. Webber, in Proceedings of the Ninth International Conference on Cosmic Rays, London, 1965 (The Institute of Physics and the Physical Society, London, 1966), Vol. 1, p. 345.

[23]The line labelled as $1/\beta$ in Fig. 1 of Ref. 22 is actually $1/\beta^2$ since the log scales differ by a factor of 2 for the two axes.

HYDROMAGNETIC WAVES IN THE INTERPLANETARY PLASMA

Paul J. Coleman, Jr.
Institute of Geophysics and Planetary Physics, University of California, Los Angeles, California
(Received 25 April 1966; revised manuscript received 6 July 1966)

This note is a preliminary report concerning a comparison of simultaneous measurements of the plasma velocity and the magnetic field in interplanetary space. The measurements were obtained with the positive-ion spectrometer, incorporating a cylindrical electrostatic analyzer, and the fluxgate magnetometer on board the spacecraft Mariner-II, during the period 29 August through 15 November 1962, while the spacecraft was in transit between the earth and Venus. Our purposes here are, first, to describe the properties of the simultaneous variations in the magnetic field, $\vec{B}$, and the plasma velocity, $|\vec{V}|$, and second, to show that these properties are among those expected if the variations were produced by hydromagnetic waves.

It will be convenient to employ heliocentric, spherical polar coordinates with the polar axis coincident with the sun's axis of rotation, denoted by $\vec{\Omega}_S$. Thus, at a point (r, θ, φ) the positive r direction is radially outward from the sun to the point, the φ direction is the direction of $\vec{\Omega}_S \times \vec{r}$, and the θ direction completes the usual right-handed system. In this system, the variables measured by the magnetometer are B_r, B_θ, and B_φ, and the variable measured by the plasma probe is $V \simeq V_r$.

As the first step in a statistical analysis of the data, amplitude distributions of these variables were examined. It was found that the distributions were roughly Gaussian. Next, using the usual methods applicable to time series that exhibit Gaussian amplitude distributions,

Table I. Ratios of the power densities, coherences squared, and phase differences obtained from six sets of auto and cross spectra for the measured variables B_r, B_θ, B_φ, and V_r. The power densities, P, the coherences squared, R, and the phase differences, Φ, are averages taken over the frequency range 1-50 cycles per day. The quantity R_{min} is the value of R required for a significant measurement of Φ, i.e., for a measurement in which the rms uncertainty of Φ is 45°. A positive polarity is assigned if the average field was directed outward from the sun; a negative polarity is assigned if it was inward toward the sun.

Period, days	Polarity	$P(B_r)/P(V_r)$	$P(B_\theta)/P(V_r)$	$P(B_\varphi)/P(V_r)$	$R(V_r,B_r)$	R_{min}	$\Phi(V_r,B_r)$ (deg)
		(10^{-23} G^2 cm^{-2} sec^2)					
243-252	+	11.8	16.5	14.5	0.223	0.021	181 ±7
254-263	−	7.8	21.2	13.4	0.050	0.023	−4 ±14
270-279	+	2.3	5.3	4.2	0.039	0.019	172 ±8
282-291	−	14.4	31.7	29.3	0.378	0.023	4 ±4
297-303	+	6.6	16.4	14.6	0.487	0.029	179 ±4
313-318	−	46.1	32.3	32.3	0.097	0.035	6 ±8
Average	+	6.9	12.7	11.1	0.250		177
Average	−	22.8	28.4	25.0	0.175		2
Average	Both	14.5	20.6	18.1	0.213		

power spectra were computed from several sections of the records for each of the four variables, and cross spectra were computed for all pairs of these four variables. The frequency range from 1 to 50 cycles per day (cpd) was examined initially.

Data obtained during the four ten-day periods and two six-day periods indicated in Table I were employed. During each of these six periods, the sense or polarity of the interplanetary field was nearly always that listed in Table I, wherein a positive polarity is assigned to a field outward from the sun and a negative polarity is assigned to a field inward toward the sun.

Let $P(X)$ be the power density at a particular frequency, f, obtained from the power spectrum of the variable X. We will be interested in the power-density ratios $P(B_r)/P(V_r)$, $P(B_\theta)/P(V_r)$, and $P(B_\varphi)/P(V_r)$. These ratios are plotted versus frequency in Fig. 1. Note that the values for each section are roughly independent of frequency.

Let $|R(X,Y)|$ be the magnitude of the square of the coherence at a particular frequency, obtained from the cross spectrum for a particular pair of variables (X, Y). Similarly, let $\Phi(X,Y)$ be the phase difference at a particular frequency obtained from the cross spectrum for the same pair of variables.

Cross spectra were computed, from the same six sections of the records, for all pairs of the measured variables. On the average, all pairs exhibited significant coherences although $|R(V_r,B_r)|$ was greater by factors in the range from 5 to 8 than the values of $|R|$ for the other pairs. The mean values of $|R(V_r,B_r)|$, taken over the frequency range 1-50 cpd, are listed in Table I. These averages are sufficient for our purposes, but the coherences generally were not strictly independent of frequency in this range.

The relatively high values of $|R(V_r,B_r)|$ resulted in relatively accurate estimates of $\Phi(V_r, B_r)$. The mean values of $\Phi(V_r,B_r)$ are also listed in Table I. The values of $\Phi(V_r,B_r)$ were strictly independent of frequency. The cross spectra for the other pairs of variables suggest that Φ was generally frequency independent, but the lower coherences in these cases preclude a more definite statement at present. Note that $\Phi(V_r,B_r) \simeq 180°$ whenever the average field was directed outward from the sun (+), and $\Phi(V_r,B_r) \simeq 0°$ whenever the average field was directed toward the sun (−).

In order to compare the properties of the auto and cross spectra of the measured variables with the properties that would be expected for variations produced by hydromagnetic waves, a simplified model for hydromagnetic waves was employed. Following Thompson,[1] we considered plane waves in the plasma displacement, $\vec{d}$, moving through a uniform, perfectly conducting, isentropic, ideal gas in a constant, uniform magnetic field, $\vec{B}_0$, for the case in which the gas is moving with a constant, uniform bulk velocity, $\vec{V}_0$. Since $\vec{V}_0$ is uniform, we may treat the system in the reference frame moving with this velocity. The transformation back to the

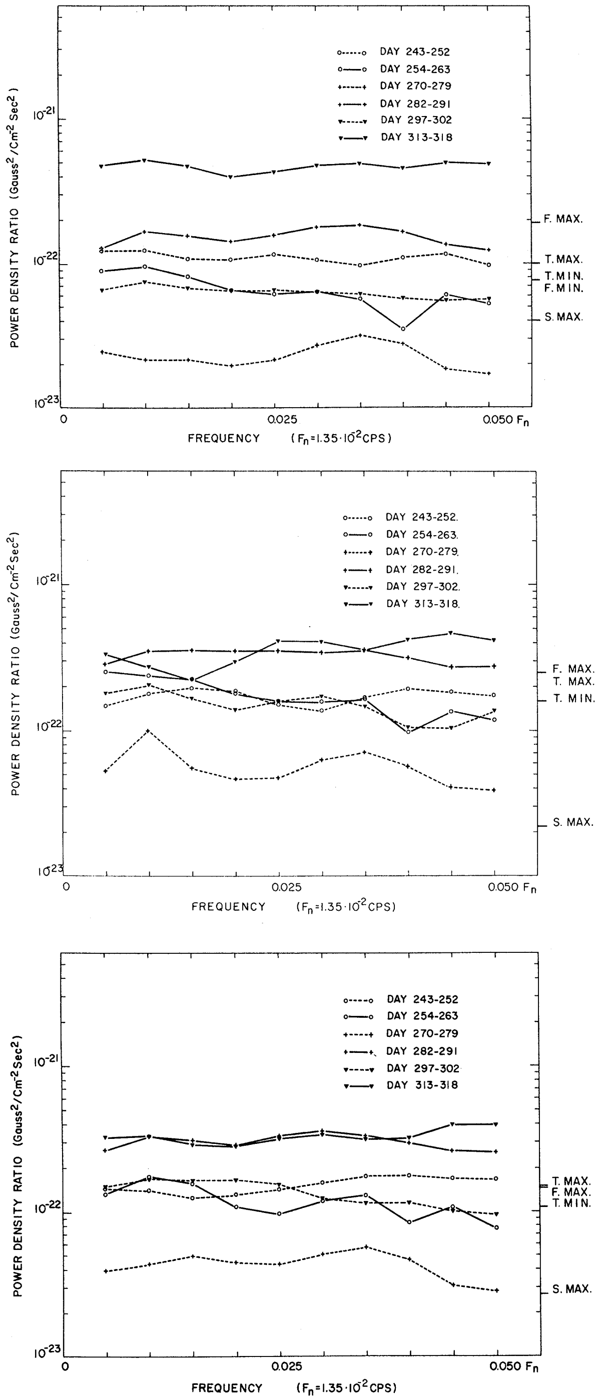

FIG. 1. Ratios of power densities. The ratio of the power density in the auto spectrum of each vector field component, B_r, B_θ, and B_φ, to the power density in the auto spectrum of the radial component of the plasma velocity, V_r, is plotted versus frequency for six sets of auto spectra. The theoretically allowed ranges for each ratio are also indicated on the right-hand side of the corresponding plot. Separate ranges are shown for each mode of propagation, fast (F), slow (S), and Alfvén or transverse (T).

inertial reference frame simply produces a Doppler shift in the frequencies of the plane waves that are under consideration here.

The linearized equations are then

$$\partial\rho/\partial t + \rho_0 \nabla\cdot\vec{v} = 0, \tag{1}$$

$$\rho_0(\partial\vec{v}/\partial t) = -\nabla p + (1/4\pi)(\nabla\times\vec{b})\times\vec{B}_0, \tag{2}$$

$$\partial p/\partial t - (\gamma p_0/\rho_0)(\partial\rho/\partial t) = 0, \tag{3}$$

$$\vec{E} + (\vec{v}/c)\times\vec{B}_0 = 0, \tag{4}$$

$$(1/c)\partial\vec{b}/\partial t = -\nabla\times\vec{E}, \tag{5}$$

where ρ_0 is the mean density and ρ is the density perturbation, $\vec{V} = \vec{V}_0 + \vec{v}$ is the velocity, $\vec{B} = \vec{B}_0 + \vec{b}$ is the magnetic field, p_0 is the mean pressure and p is the pressure perturbation, $\vec{E}$ is the electric field, γ is the ratio of specific heats for the ideal gas, and c is the velocity of light.

Now from the equations given above, it can be shown that there are three modes in which plane waves can propagate. Still following Thompson,[1] we will designate these modes as the Alfvén mode, the fast mode, and the slow mode.

In describing the orientation of $\vec{B}_0$, we will use the angles $\alpha = \tan^{-1}(-B_\varphi/B_r)$ and $\beta = \tan^{-1}[B_\theta/(B_r^2 + B_\varphi^2)]$. In describing the orientation of the propagation vector, $\vec{k}$, of a plane wave, we will use θ_k, the angle from the line of force corresponding to $\vec{B}_0$ to $\vec{k}$. This angle is always measured from the direction outward from the sun along this line of force. We will denote by φ_k the angle that defines the direction of $\vec{k}_\perp$, the component of $\vec{k}$ transverse to $\vec{B}_0$.

For any allowed plane wave, the orientation of $\vec{k}_\perp$ and $\vec{B}_0$ determine the orientation of the plane of polarization of the wave. We treated the case of a superposition of many plane waves with random phases and with the orientations of the planes of polarization distributed uniformly over the allowed range.

For any such distribution of plane waves, in any of the three modes that satisfies the system of Eqs. (1)-(5), the power-density ratios, the coherences, and the phase differences depend upon the phase velocity, U, the mean field strength, B_0, the direction of propagation relative to $\vec{B}_0$ given by (θ_k, φ_k), and the orientation of $\vec{B}_0$ given by (α, β). The phase velocity, in general, depends upon θ_k, B_0, ρ_0, and the temperature T.

Values of $P(B_i)/P(V_r)$ $(i = r, \theta, \varphi)$, $|R(V_r, B_r)|$, and $\Phi(V_r, B_r)$, computed for the idealized waves are listed in Table II for the following 63 cases:

Table II. Results of calculations of power-density ratios, coherences squared, and phase differences for idealized hydromagnetic waves. In these calculations, $B_0 = 5\times10^{-5}$ G, $n = 5$ protons/cm^3, $T = 10^5$ °K. The phase difference, Φ, between a pair of variables is given by the sign of R, the square of the coherence, for the pair. Thus, the pair is in phase for $R > 0$, and 180° out of phase for $R < 0$. Where two signs are given, the upper sign corresponds to the case of $\beta = 25°$, and the lower sign is for $\beta = -25°$. The quantity P for a particular variable is just the average power that would appear in a record of the variable that was one period of oscillation in length. In these calculations, it was assumed that the variations would be produced by a superposition of randomly polarized waves. For transverse waves the range of θ_k indicated by "all" is $0 \leq \theta_k \leq 90°$. The results given here are for the case $\vec{k}\cdot\vec{B}_0 > 0$. For $\vec{k}\cdot\vec{B}_0 < 0$, all phase differences change by 180°.

θ_k (deg)	$P(B_r)/P(V_r)$	$P(B_\theta)/P(V_r)$ (10^{-23} G^2 cm^{-2} sec^2)	$P(B_\varphi)/P(V_r)$	$R(V_r,B_r)$	$\Phi(V_r,B_r)$ (deg)
		Slow mode, $\beta = 0°$			
0	0.00	0.00	0.00	0.00	···
15	0.58	1.17	0.76	−0.55	180
30	1.48	1.83	1.58	−0.82	180
45	2.35	1.48	2.10	−0.93	180
60	3.12	0.79	2.43	−0.98	180
75	3.65	0.22	2.64	−0.99	180
90	3.84	0.00	2.71	−1.00	180
		Slow mode, $\beta = \pm25°$			
0	0.00	0.00	0.00	0.00	···
15	0.83	1.19	1.00	−0.52	180
30	1.84	2.06	1.95	−0.78	180
45	2.64	2.10	2.39	−0.91	180
60	3.28	1.82	2.59	−0.97	180
75	3.70	1.54	2.68	−0.99	180
90	3.84	1.42	2.71	−1.00	180
		Fast mode, $\beta = 0°$			
0	10.50	25.40	14.90	−1.00	180
15	9.08	18.30	11.80	−0.66	180
30	9.74	12.10	10.40	−0.30	180
45	12.20	7.71	10.90	−0.11	180
60	15.30	3.90	12.00	−0.02	180
75	17.90	1.07	12.90	0.00	···
90	18.90	0.00	13.30	0.00	···
		Fast mode, $\beta = \pm25°$			
0	10.50	16.60	13.40	−1.00	180
15	9.08	13.10	11.00	−0.76	180
30	8.78	9.84	9.28	−0.48	180
45	9.69	7.70	8.75	−0.28	180
60	10.90	6.08	8.66	−0.15	180
75	12.00	4.98	8.69	−0.06	180
90	12.40	4.59	8.71	0.00	···
		Transverse mode, $\beta = 0°$			
All	10.00	25.00	15.10	−1.00	180
		Transverse mode, $\beta = \pm25°$			
All	7.70	16.00	10.80	−1.00	180

fast, slow, and Alfvén modes, and values of 0, 15, 30, 45, 60, 75, and 90° for θ_k, 40° for α, 0° and ±25° for β, 5.0×10^{-5} G for B_0, $5m_p$ cm^{-3} (m_p = 1 proton mass) for ρ_0, and 10^5 °K for T.

The parameters used here to describe the unperturbed medium are based upon averages recorded during the flight of Mariner-II. The average value of the field strength B_0 was 5γ $= 5\times10^{-5}$ G. The angle α was typically 40° when the field was outward from the sun, and the angle β was typically in the range ±25°. According to Neugebauer and Snyder,[2,3] the average proton number density, n_p, was 5 cm^{-3}, and the average proton temperature, T, was 1.7×10^5 °K. The average ion velocity, V_0, was about 500 km/sec. The values given in Table II correspond to situations in which $\vec{B}_0\cdot\vec{k} > 0$. For

$\vec{B}_0 \cdot \vec{k} < 0$, the values of $\Phi(V_\gamma, B_\gamma)$ would differ by 180° from those listed, but the power-density ratios and coherences for the ideal waves depend upon $|\vec{B}_0 \cdot \vec{k}|$ rather than $\vec{B}_0 \cdot \vec{k}$.

We expect this model to be useful for describing waves with frequencies well below the positive-ion gyro frequency, which is 0.08 cps for a proton in a 5-γ field. For a plasma moving with a bulk velocity $V_0 \simeq 500$ km/sec, waves with this frequency could produce variations in $\vec{V}$ and $\vec{B}$ with frequencies in the range from the ion gyro frequency to 1 or 2 cps, due to Doppler shifts.

Let us now turn to the comparison of the properties of the observed variations with the properties of the variations that would be expected in the ideal case. The measured and ideal power-density ratios $P(B_i)/P(V_\gamma)$ may be compared in Fig. 1. In no cases do the measured values exceed three times the maxima of the theoretically allowed ranges.

We conclude from this comparison that waves propagating in either the Alfvén mode or the fast mode, or both, were present. However, the presence of waves in the slow mode cannot be established because the magnetic effects of slow waves are considerably weaker than those of either of the other two modes.

Power spectra of the variations of the vector component of the field along $\vec{B}_0$ have also been computed. These spectra are quantitatively similar to those of B_γ. Since Alfvén waves would produce no variations along $\vec{B}_0$, waves in the fast mode were evidently present. At this point, we cannot determine whether Alfvén waves were present as well.

From Fig. 1, it is apparent that the measured power-density ratios are frequency independent. According to the model, frequency independence is expected if the amplitudes of the waves in one mode relative to the amplitudes of the waves in each of the other modes are roughly the same at any of the frequencies studied.

Under this condition, the phase differences are also expected to be independent of frequency, just as observed. If the waves propagate predominantly outward from the sun, we would expect $\Phi(V_\gamma, B_\gamma) = 180°$ for (+) and 0° for (−). This is just the situation that was observed, as shown in Table I.

The measured values of the square of the coherence, $|R(V_\gamma, B_\gamma)|$, given in Table I, are somewhat lower than most of the values given in Table II. However, even if outwardly propagating waves predominate, any contribution from inwardly propagating waves would reduce the coherence. We also remarked earlier that the coherences showed some dependence upon frequency. Such a dependence could appear, even though the power-density ratios and phase differences are frequency independent, if the power spectra of the inward and outward bound waves were somewhat different.

I wish to express my appreciation to M. M. Neugebauer and C. W. Snyder for permission to use data from the Mariner-II plasma probe; and to L. Davis, Jr., C. P. Sonett, and E. J. Smith with whom I collaborated on the Mariner-II magnetometer experiment. This work was supported by the National Aeronautics and Space Administration under Research Grant No. NsG 249.

[1]W. B. Thompson, An Introduction to Plasma Physics (Pergamon Press, New York, 1962), Chap. 5.

[2]M. M. Neugebauer and C. W. Snyder, Science 138, 1 (1962).

[3]M. M. Neugebauer and C. W. Snyder, to be published.